Electrocatalytic reduction of Nitrate on Copper single crystals in acidic and alkaline solutions.

Elena Pérez-Gallent, Marta C. Figueiredo, Ioannis Katsounaros, Marc T.M. Koper*

Leiden Institute of Chemistry, Leiden University, PO Box 9502, 2300 RA Leiden, The Netherlands

ARTICLE INFO

ABSTRACT

Nitrate reduction on Cu (100) and Cu (111) surfaces in alkaline and acidic solutions was studied by electrochemical methods (cyclic voltammetry, rotating disc electrode) coupled with online and in situ characterization techniques (mass spectrometry, ion chromatography and Fourier transformed infra-red spectroscopy) to evaluate the reaction mechanism and products on the different surfaces. Electrochemical results show that reduction of nitrate in alkaline media on Cu is structure sensitive. The onset potential on Cu (100) is +0.1 V vs. RHE, ca. 50 mV earlier than on Cu (111). The onset potentials for nitrate reduction on Cu (100) and Cu (111) in acidic media are rather similar. Analytical techniques show a diverse product distribution for both surfaces and for both electrolytes. Whereas in acidic media both Cu electrodes show the formation of NO and ammonia, in alkaline media Cu reduces nitrate to nitrite and further to hydroxylamine. In alkaline media, Cu (100) is a more active surface for the formation of hydroxylamine than Cu (111).

1. Introduction

Human activities like the combustion of fossil fuels, the nuclear industry, the production of nitrogen fertilizers and the cultivation of nitrogen-fixing plants are inducing severe alterations in the global nitrogen cycle [1]. The rate of many human-caused global changes has increased severely in last decades, but none so rapidly as industrial production of N fertilizers, which has grown exponentially since the 1940s. The increase of the availability of N also increases biomass production and accumulation significantly [2]. Consequently, changes in nitrogen cycle can also lead to changes in the global carbon cycle, generating an increase of carbon dioxide in the atmosphere [3]. The slow natural process of denitrification is unable to deal with the surplus of nitrate-derived compounds leading to a deteriorating effect on our ecological system and human health.

Electrochemistry could play an important role in the development of new denitrification technologies due to its environmental compatibility, versatility, energy efficiency, selectivity and low associated costs, as well as the non-requirement of reduction agent [4,5]. However, there is a need for an appropriate electrocatalyst that can provide an optimized process with high selectivity to harmless products like N_2 or valuable products such as ammonia or hydroxylamine. The electrochemical reduction of nitrate has been studied on several transition and coinage metal electrodes in acidic media [4]. Copper has been shown to be the most active coinage metal for this reaction having ammonia as main product [6,7]. A high electrochemical activity for nitrate reduction has also been observed on copper electrodes in alkaline solutions [8]. Nitrate reduction in alkaline media is of interest due to the less probable solution-phase formation of products like toxic nitrogen oxides [9], as compared to reduction in acidic media, and because of the concern of removing nitrate from alkaline nuclear waste. In this context, the use of single-crystal copper surfaces offers the unique opportunity to evaluate the effect of the surface atomic structure on the reaction rate, the preferred reaction paths and the resulting product distribution [10].

In this work, we study the influence of the surface structure of Cu electrodes on the nitrate reduction in alkaline and acidic media. We use electrochemical techniques (cyclic voltammetry, rotating disc electrode) coupled with online and in situ characterization techniques (mass spectrometry, ion chromatography and Fourier transformed infra-red spectroscopy) to evaluate the reaction mechanism and products on the different surfaces and their dependence on the available atomic sites.

* Corresponding author.
E-mail address: m.koper@chem.leidenuniv.nl (M.T.M. Koper).

2. Experimental

Prior to each electrochemical experiment, the glassware used was stored overnight in a solution of $KMnO_4$ that was rinsed with a mixture of ultra clean water (Millipore MilliQ, resistivity > 18.2 $M\Omega$), 20 mL/L of hydrogen peroxide and 1 mL/L of concentrated sulfuric acid. The glassware was further cleaned by boiling 4 times in Millipore MilliQ water. A coiled platinum wire was used as a counter electrode and a reversible hydrogen electrode (RHE) in the same electrolyte was used as the reference electrode. All potentials in this paper are referred to RHE.

The copper electrodes used were 99.99% copper disks with a diameter of 6 mm, purchased from Mateck and aligned to $< 0.5°$ accuracy. Prior to every experiment, the electrodes were electro-polished in a 10:5:2 mixture of H_3PO_4:H_2O:H_2SO_4 at +3 V vs. Cu for 30 s, followed by a stabilization step at 0 V for 30 s. After thorough rinsing with ultrapure water, the surface of the crystal was characterized by cyclic voltammetry at a scan rate of 50 mV/s in NaOH 0.1 M solution[11]. Cyclic voltammograms were recorded by an Ivium A06075 potentiostat.

Electrolytes were made from ultra-pure water (Millipore MilliQ, resistivity $> 18.2\,M\Omega$) and high purity reagents (Sigma Aldrich TraceSelect). Before every experiment, Argon (Linde, 6.0) was bubbled through the electrolyte for 15 min in order to remove air from the solution, and during the experiments the argon was kept flowing above the solution.

In order to control mass transfer rates, Cyclic Voltammetry (CV) under hydrodynamic conditions was performed with a home-made hanging-meniscus rotating disc electrode (HMRDE) configuration, compatible with single-crystal electrodes. The rotation was controlled with a modulated speed rotator (PINE, MSR). Experiments were carried out at a rotation rate of 400 rpm.

Online Electrochemical Mass Spectroscopy (OLEMS)[12] was used to detect the gaseous products formed during the reaction. The reaction products at the electrode surface were collected by a hydrophobic Teflon tip situated very close to the surface of the electrode (about 10 μm). The tip is a 0.5 mm diameter porous Teflon cylinder with an average pore size of 10–14 μm in a Kel-F holder, connected to a mass spectrometer by a PEEK capillary. Before every experiment, the tip was submerged in a solution of 0.2 M $K_2Cr_2O_7$ in 2 M H_2SO_4 and rinsed extensively with MilliQ water. A Balzers Quadrupole mass spectrometer with a secondary electron multiplier (SEM) voltage of 2400 V was used for the detection of every mass. The different mass signals were followed while changing the electrode potential from +0.25 V to −1 V vs. RHE and back at a scan rate of 1 mV/s.

Online Ion Chromatography (IC) was utilized to detect ionic products dissolved in the electrolyte[13]. The reaction products were collected with an automatic sample collector (FRC-10A, Shimadzu) by an open tip situated very close (about 10 μm) to the electrode. The potential of the electrode was changed from 0.35 V to −0.6 V and back at a scan rate of 1 mV/s. Every sample contains 60 μL and they were collected with a rate of 60 μL/min, meaning that every sample contains the average products of a change in potential of 60 mV. After voltammetry, all the samples collected were analyzed with IC (Shimadzu, Prominence) equipped with a conductivity detector (CDD-10A vp, Shimadzu). For the detection of the anion (NO_2^-), sodium nitrite (Merck, 99.99%) was utilized to prepare standard solutions, from which the retention time was determined and the concentration was calibrated. An NI-424 (Shodex) anionic column was used at a constant temperature of 40 °C with an eluent flow rate of 1 mL/min. The eluent consists of 2.8 mM BIS-TRIS (Fluka, BioXtra, >99%), 2 mM phenylboronic acid (Fluka, purum, >97%), 8 mM 4-hydroxybenzoic acid (Sigma-Aldrich, 99%), and 0.005 mM trans-1,2-diaminocyclohexane-N,N, N′,N′-tetra acetic acid (Sigma- Aldrich, ACS reagent, >99%).

In all the above techniques, the electrode was in hanging meniscus configuration, meaning that only the face of the crystal with the desired structure was in contact with the electrolyte.

FTIR measurements were performed with a Bruker Vertex 80 V Infrared spectrophotometer[14]. The electrochemical cell was assembled on top of a 60° CaF_2 prism, and the electrode was situated against this prism to form a thin layer. The measurements were performed under external reflection. FTIR spectra were obtained from an average of 100 scans with a resolution of 8 cm^{-1} at the selected potentials. Every spectrum was obtained by applying single potential steps compared to the reference potential (+0.35 V vs. RHE). The spectra are shown as (R-R$_0$/R$_0$) where R is the reflectance at the sample potential and R$_0$ is the reflectance at the reference potential. Thereby the ratio $\Delta R/R_0$ gives positive bands for the formation of species at the sample potential, and negative bands correspond to the loss of species at the sample potential. P-polarized light was used to probe species both near the electrode surface and in solution.

3. Results and Discussion

3.1. Nitrate reduction in alkaline media

3.1.1. Cyclic voltammetry (CV) and hanging-meniscus rotating disc electrode (HMRDE) measurements

Fig. 1a shows the cyclic voltammograms for Cu (111) (blue curve) and Cu (100) (green curve) in 0.1 M NaOH solution (dashed lines) and in 0.1 M NaOH with 2 mM of $NaNO_3$ (full lines). In the blank voltammetry, for both surfaces we observe a featureless voltammogram between +0.3 V and −0.5 V vs. RHE. When more negative potentials are applied, both surfaces evolve hydrogen, with Cu (111) being more active for HER with an onset potential of −0.4 V compared to −0.5 V for Cu (100). With nitrate in solution, reduction currents are observed for both surfaces at much lower potentials than HER. Cu (111) shows two reduction peaks, the first one starts at +0.15 V reaching a maximum current density of ca. −0.4 mA/cm^2 at +0.1 V. The second peak has an onset potential of −0.15 V reaching a maximum current density of ca. −3 mA/cm^2 at −0.5 V. On the other hand, Cu (100) shows one peak starting at +0.1 V reaching a maximum current density of ca. −4.3 mA/cm^2 at
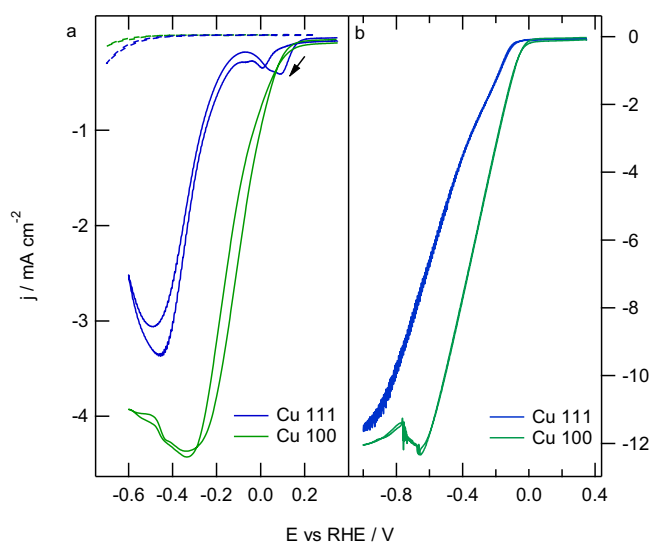

Fig. 1. Cyclic voltammetry recorded at Cu (111) and Cu (100) electrodes in 0.1 M NaOH in the absence (dashed lines) and presence (solid lines) of a) 2 mM $NaNO_3$ and b) 10 mM $NaNO_2$ Experimental conditions: scan rate 50 mV/s; rotation rate 400 rpm (For interpretation of the references to colour in text, the reader is referred to the web version of this article.).

−0.3 V. According to the literature [6,15–17] the first reduction product of nitrate reduction is nitrite. The small reduction peak starting at +0.15 V on the Cu (111) electrode is probably associated with this first reduction step:

$$NO_3^- + H_2O + 2e^- \rightarrow NO_2^- + 2\ OH^- \tag{1}$$

as is evidenced by the absence of this peak when the reactant is NaNO₂ (see Fig. 1b). The voltammogram obtained with Cu (100) only shows one wave with an onset potential of +0.1 V, associated with the formation of nitrite and further reduced products as suggested by the CVs for nitrite reduction shown in Fig. 1b. Cu (100) shows a diffusion-limited plateau with a maximum current density of ca. −4.3 mA/cm² at around −0.3 V, this limiting current being dependent on rotation rate. A Levich plot of the rotation-rate dependence of the current plateau is not perfectly linear; from the slope we estimate that the number of electrons involved in the process is between 5 and 7 (with 6 corresponding to the formation of hydroxylamine). On the other hand, the CV obtained for Cu (111) is only partially diffusion limited and does not reach a plateau current. Although on Cu (111) the reduction of nitrate has a lower onset potential, the reaction appears to become blocked by intermediates of the hydrogen evolution reaction, which has a more positive onset potential on Cu (111) than on Cu (100), and as a result the nitrate reduction is not able to reach full diffusion limitation on Cu (111).

We note that in the presence of nitrate there is a strong poisoning effect on Cu (111) as illustrated in Fig. 2, showing cyclic voltammograms of the nitrate reduction reaction as a function of the cycle number for Cu (100) (Fig. 2a) and Cu (111) (Fig. 2b) electrodes in a 0.1 M NaOH solution containing 2 mM NaNO₃. The reduction peak observed at +0.15 V in the first cycle of nitrate reduction on Cu (111) is absent in the following cycles, suggesting that the reaction on Cu (111) is inhibited already after the first cycle. Both electrodes show deactivation with cycling in the potential window shown in Fig. 2, but the deactivation of the Cu (111) electrode is much more pronounced than for Cu (100). If the negative vertex of the potential window is limited to −0.4 V (see Fig. 3a), Cu (100) does not show deactivation, suggesting that the deactivation is associated with the formation of adsorbed hydrogen. On the contrary, Cu (111) still shows deactivation also

if the potential scan is limited to −0.4 V (see Fig. 3b), in agreement with the lower onset potential for hydrogen evolution and hydrogen adsorption on Cu (111). This inhibition and deactivation by adsorbed hydrogen is also known for nitrate reduction on Pt [17,18]. Similarly to nitrate reduction on Pt the negative differential resistance that is the result of the inhibition by adsorbed hydrogen can give rise to spontaneous (current) oscillations [19] during nitrate reduction, as illustrated in Fig. 2a for Cu (100). These oscillations are caused by the interplay between the negative differential resistance and the ohmic resistance of the electrolyte solution [20]. The possibility of poisoning of the electrode by intermediate N-containing species was also considered. However, we consider it less likely considering that self-poisoning typically does not lead to a negative differential resistance, but rather to a lower overall current. The observed negative differential resistance is characteristic for poisoning by a parallel side reaction, in this case hydrogen adsorption.

3.1.2. Ion Chromatography and OLEMS data

Fig. 4 illustrates the formation of nitrite detected by Ion Chromatography as a function of the cycle number for Cu (100) (Fig. 4a) and Cu (111) (Fig. 4b) in a 0.1 M NaOH solution containing 2 mM NaNO₃. The onset potential for the formation of nitrite matches the onset potential seen in voltammetry (see Fig. 1), i.e. +0.15 V for Cu (111) and +0.1 V for Cu (100). The profile of the formation of nitrite on Cu (100) shows a maximum at −0.1 V, and decreases at more negative potentials, indicating the further reduction of nitrite. On the other hand, the formation of nitrite on Cu (111) shows a less accentuated profile, with a plateau, suggesting that further reduction is slow. Moreover, consistent with the deactivation of Cu (111) shown in Fig. 2, Cu (111) does not form any nitrite in the second cycle of the voltammetry, whereas Cu (100) shows only a small decay in the amount of nitrite formed compared with the amount formed in the first cycle. Note, however, that the employed scan rate in Fig. 4 is significantly lower than in Figs. 2 and 3. We note that the detection of nitrite with IC was stable over time and no decomposition of nitrite in alkaline media was observed.

The possible formation of gaseous products such as N₂O, NO or N₂ during the reduction of nitrate, was followed by OLEMS. As
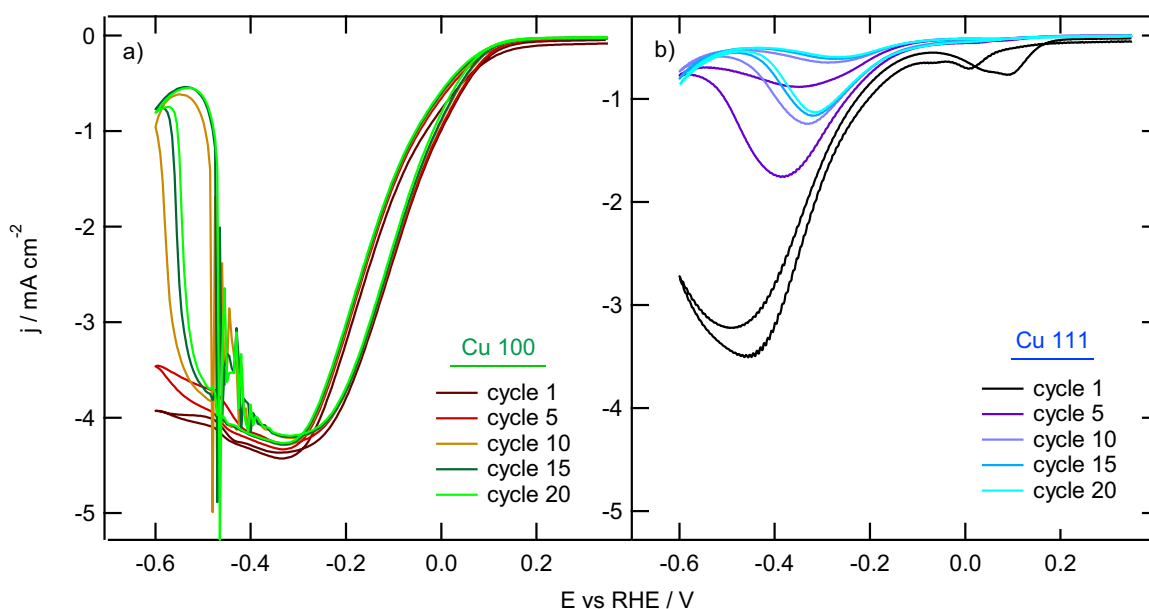

Fig. 2. Cyclic voltammetry recorded at a) Cu (100) and b) Cu (111) electrodes in 0.1 M NaOH in the presence of 2 mM NaNO₃ as a function of the cycle number. First cycle starts at 0.35 V vs. RHE. Experimental conditions: scan rate 50 mV/s; rotation rate 400 rpm.
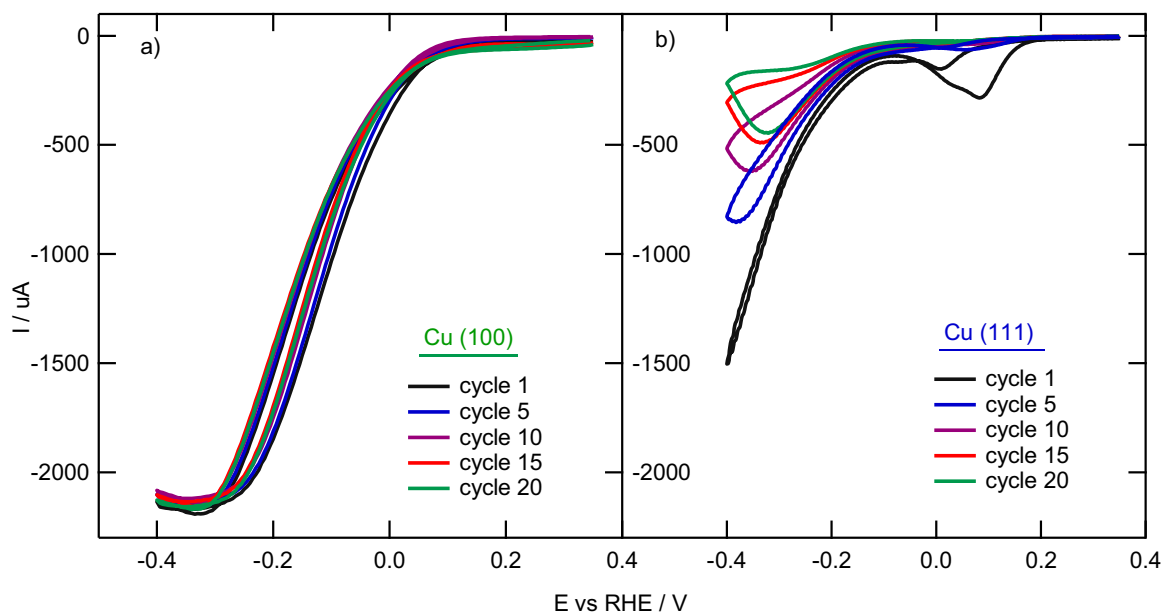
Fig. 3. Cyclic voltammetry recorded at a) Cu (100) and b) Cu (111) electrodes in 0.1 M NaOH in the presence of 2 mM NaNO$_3$ in the potential window between +0.35 and −0.4 V vs. RHE as a function of the cycle number. Experimental conditions: scan rate 50 mV/s; rotation rate 400 rpm.
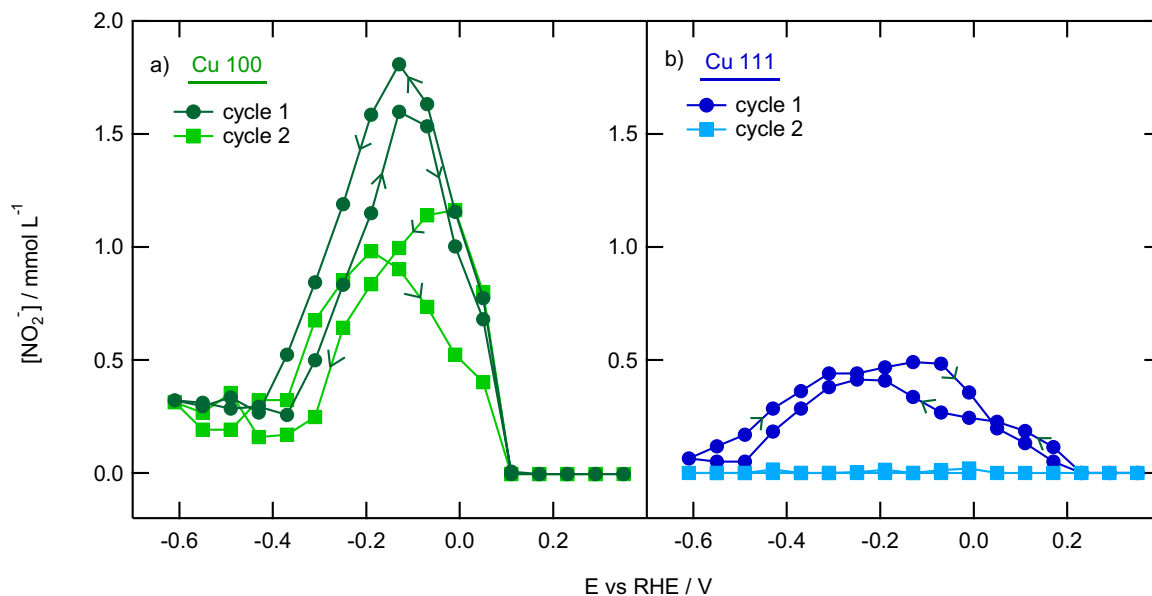

Fig. 4. Formation of NO$_2^-$ detected with online ion chromatography from a) Cu (100) electrode and b) Cu (111) electrode in a 0.1 M NaOH solution containing 10 mM NaNO$_3$. Scan rate = 1 mV/s.

Fig. 5 shows, neither Cu (111) nor Cu (100) form any gaseous products other than hydrogen, which is associated with the reduction of water from the electrolyte.

3.1.3. FTIR spectroscopy

Reaction intermediates or possible adsorbates on the electrodes were followed by FTIR in order to obtain a better insight about the intermediates and the mechanism of the reaction. Fig. 6 displays the potential dependent absorbance spectra with respect to the reference potential (0.35 V). In agreement with the onset potentials for nitrate reduction observed in the CVs (Fig. 1) and IC (Fig. 4), the absorbance spectra also show that the onset potential for the reduction of nitrate is 0.15 V on Cu (111) and +0.1 V on Cu (100), as observed by a negative band at 1370 cm^{-1}

associated with the consumption of nitrate[14]. Simultaneously to nitrate consumption the formation of nitrite can be seen by the positive band at 1231 cm^{-1}, which appears at similar potentials to those observed by IC (Fig. 4). Interestingly, the band observed at 1191 cm^{-1} during the reduction of nitrate on Cu (100) indicates the production of hydroxylamine (NH$_2$OH) [21] at potentials more negative than 0 V (see Fig. 6 left panel). By contrast, the spectra recorded with Cu (111) do not show the band at 1191 cm^{-1}. However, cathodic currents are observed in the reduction of NaNO$_2$ on Cu (111), suggesting that nitrite can still be reduced. Fig. 1b shows similar limiting currents for both surfaces, suggesting that the reduced product has the same nature, but is formed with a slower rate on Cu (111). Therefore, we suggest that, even though clear hydroxylamine bands are not present in the FTIR spectra on
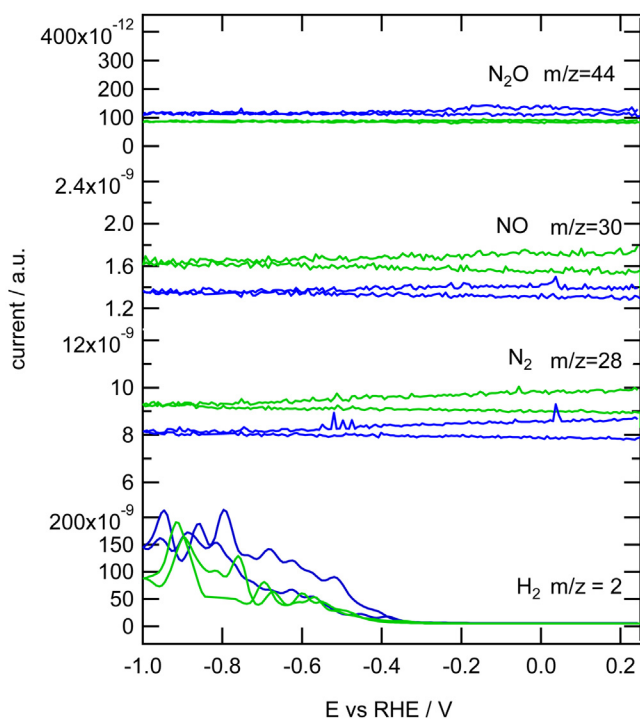
Fig. 5. Mass fragments associated with various products measured with OLEMS for the reduction of 10 mM $NaNO_3$ in 0.1 M NaOH solution in Cu (100) (green curves) and Cu (111) (blue curves) electrodes. Scan rate = 1 mV/s (For interpretation of the references to colour in this figure legend, the reader is referred to the web version of this article.).
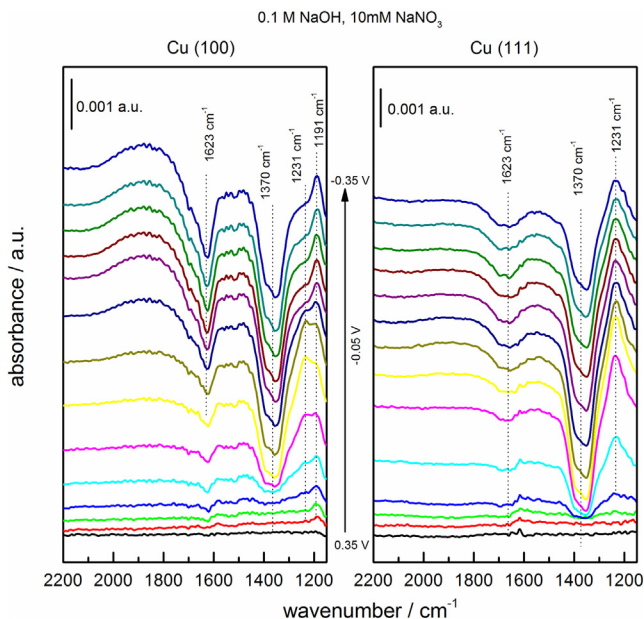

Fig. 6. Potential dependent absorbance spectra for the reduction of 10 mM $NaNO_3$ on Cu (100) (left panel) and on Cu (111) (right panel) electrode in 0.1 M NaOH solution. Reference spectrum recorded at 0.35 V vs. RHE. Potential step is 0.05 V.

Cu (111), the most likely product is still NH_2OH. The absence of the bands related to hydroxylamine in the working potential range suggests that hydroxylamine is formed with a too low concentration at potentials less negative than −0.35 V. Also, it is important to highlight the absence of adsorbed NO on both copper surfaces, even when the FTIR spectra were recorded in NaOH solution using

D_2O (See Supporting information FigsS1.). The negative band observed at 1623 cm^{-1} is due to the O-H bending of water.

The reduction of nitrite (NO_2^-) was also studied by FTIR on both copper surfaces (see Fig. 7). As the CVs in Fig. 1b show, the reduction of nitrite on Cu (100) starts ca. +0.1 V earlier than on Cu (111). Similar to nitrate reduction, also for nitrite reduction the Cu (111) electrode shows a more pronounced inhibition by hydrogen than Cu (100). FTIR spectra were taken in 0.1 M NaOH solutions containing 10 mM of $NaNO_2$ (see Fig. 7). Spectra obtained with Cu (100) show a negative band at 1235 cm^{-1} corresponding with the consumption of nitrite [22] and a positive band at 1191 cm^{-1} assigned to the formation of hydroxylamine [21]. When Cu (111) is used, the spectra only show a clear negative band at 1235 cm^{-1} corresponding to the consumption of nitrite suggesting that nitrite is indeed reduced further. A small band can be observed at 1190 cm^{-1} suggesting formation of hydroxylamine in accordance with the cathodic currents observed in the reduction of $NaNO_2$ on Cu (111).

Detection of hydroxylamine with another analytical technique such as Ion Chromatography was not technically feasible due to the chemical decomposition of hydroxylamine in alkaline media in the presence of oxygen as described by Hughes et al. [23].

3.2. Nitrate reduction in acidic media

In order to investigate the pH dependence of nitrate reduction, [8,10,16]cyclic voltammetry, OLEMS and FTIR measurements were performed in 0.1 M $HClO_4$ solution on both Cu (111) and Cu (100).

3.2.1. CV and RDE data

Fig. 8 displays the cyclic voltammograms recorded for Cu (111) and Cu (100) in a 0.1 M $HClO_4$ solution. There is a significant dependence of the profile of the CV on the surface orientation of the copper electrode. In the absence of nitrate, Cu (111) is the more active surface for HER, as in alkaline media, starting at −0.4 V on Cu (111) and at −0.5 V on Cu (100). In the presence of nitrate, the onset potential for nitrate reduction in acidic media seems to be rather similar, around +0.2 V vs. RHE, for both copper surfaces. On both electrodes the cathodic current reaches a diffusion limited plateau
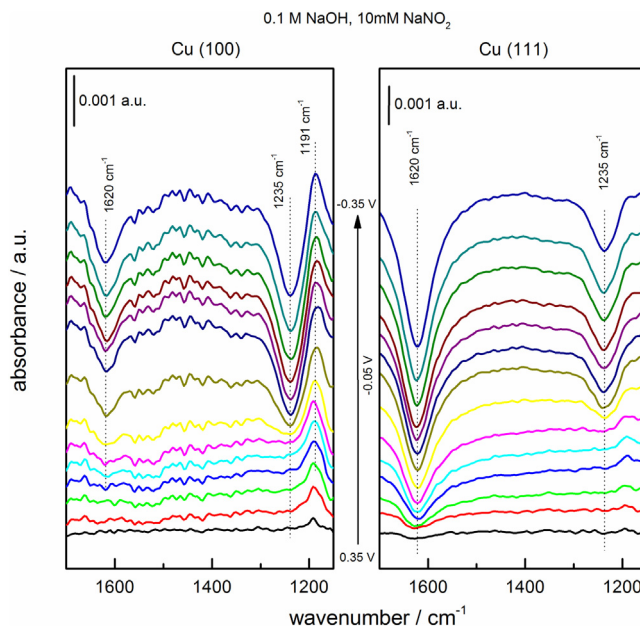

Fig. 7. Potential dependent absorbance spectra for the reduction of 10 mM $NaNO_2$ on Cu (100) (left panel) and on Cu (111) (right panel) electrode in 0.1 M NaOH solution. Reference spectrum recorded at +0.35 V vs. RHE. Potential step is 0.05 V.
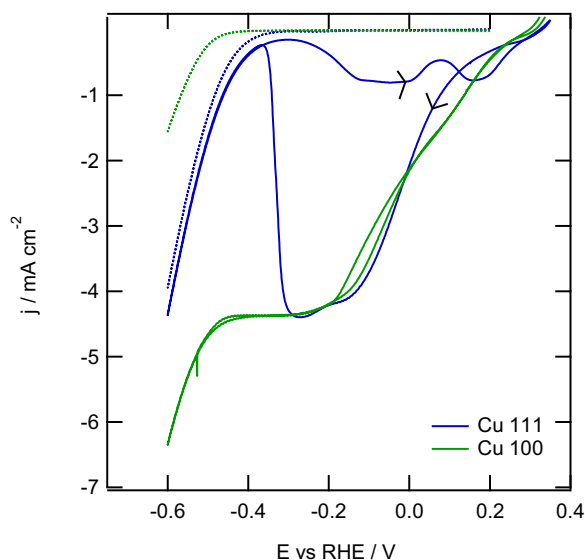
Fig. 8. Cyclic voltammetry recorded at Cu (111) (blue curve) and Cu (100) electrodes (green curve) in 0.1 M HClO$_4$ in the absence (dashed line) and presence (solid line) of NaNO$_3$. Experimental conditions: scan rate 50 mV/s; rotation rate 400 rpm; [NaNO$_3$] = 2 mM (For interpretation of the references to colour in this figure legend, the reader is referred to the web version of this article.).

at around −0.1 V. At Cu (111) the current drops drastically to a value close to zero at −0.3 V to eventually increase again at −0.4 V due to the hydrogen evolution reaction. The voltammogram for Cu (100) appears to show two waves with an inflection feature at around 0 V. The cathodic current reaches a plateau at around −0.2 V with the same current density as the plateau obtained on Cu (111), ca. −4.5 mA/cm^2. CVs recorded on Cu (100) show diffusion limited currents that depend on the rotation rate, following the Levich equation. From the slope of the Levich plot, the number of electrons involved in the process was calculated to be close to 5. From the reduction of NO$_3^-$, a 5e-transfer process would suggest formation of N$_2$. However, OLEMS measurements showed the absence of nitrogen formation, with the only volatile product being NO, as shown in Fig. 9. Cu (111) reaches the same diffusion-limited current at −0.2 V, but becomes poisoned at ca. −0.3 V, probably due to the blockage of the surface by adsorbed hydrogen.

Cyclic voltammograms recorded on Cu (111) and on Cu (100) in a 0.1 M HClO$_4$ solution containing 2 mM NaNO$_3$, as a function of the cycle number, are plotted in Fig. 10. The evolution of the CVs differs between the two surfaces. On Cu (111) (right panel) the features a, b and c give rise to a more negative currents with increasing number of cycles, and the decay in current observed at −0.3 V in the first cycle is shifted to more positive potentials in subsequent scans. The exact reason for the time evolution of the cycles in Fig. 10b is not known. On Cu (100), there is no strong effect of repeated cycling and no deactivation. In line with the greater extent of deactivation of Cu (111) in alkaline media, in acidic media Cu (111) also shows a much stronger deactivation than Cu (100) for the reduction of NO$_3^-$. However, the CV on Cu (111) shows no deactivation if the negative potential limit is kept above −0.2 V (see Fig. 11), suggesting that the cause of the deactivation is adsorbed hydrogen. As mentioned above, the deactivation of Pt electrode during nitrate reduction has also been suggested to be related to the formation of H$_{ads}$ [17].

3.2.2. FTIR spectroscopy

With the aim to elucidate possible adsorbates or intermediates of the reaction, FTIR measurements were carried out on both copper electrodes in 0.1 M HClO$_4$ solution. Fig. 12 shows the
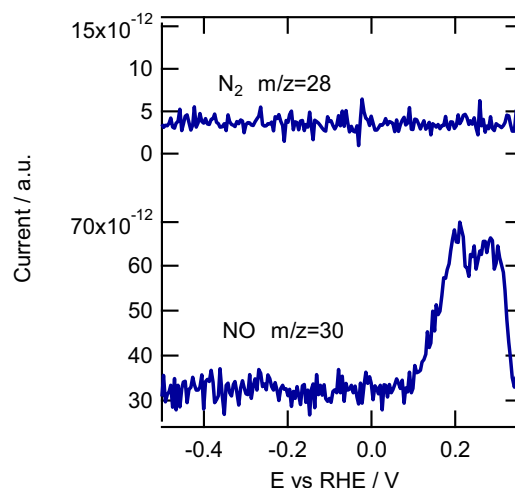

Fig. 9. Mass fragments associated with various products measured with OLEMS for the reduction of 10 mM NaNO$_3$ in 0.1 M HClO$_4$ solution on a Cu (100) electrode. Scan rate = 1 mV/s.

potential dependent absorbance spectra with respect to the reference potential of +0.35 V. The FTIR spectra indicate that the onset potential for nitrate reduction in acidic media is +0.15 V for Cu (100) and +0.1 V for Cu (111) as shown by the negative bands at 1270 cm^{-1} associated with the consumption of nitrate [14]. These values of the onset potential are in agreement with the values observed with cyclic voltammetry (see Fig. 8). Interestingly, the band corresponding to nitrite is not present in the spectra, probably because of the fast conversion of nitrite into NO in acidic media, and subsequent reduction of NO to ammonium [9,17]. N-O stretching bands corresponding to adsorbed NO are present in the spectra of both electrodes. On Cu (111), the band appears at 1627 cm^{-1} [24] and on Cu (100) the band appears at 1617 cm^{-1} [25]. The onset potential for the formation of NO is difficult to estimate, since the small NO band is hidden in a fluctuation of the baseline of the spectra due to changes in the thin layer. Both copper surfaces show a positive band at 1460 cm^{-1} corresponding to NH$_4^+$ [14]. Ammonium formation starts around +0.1 V vs. RHE for both copper orientations. These observations are consistent with the results by Bae et al. [10,15], who reported the formation of NO and ammonium for the reduction of nitrate on copper.

3.3. General Discussion

From the above results, we conclude that there are both structural and pH effects for nitrate reduction on copper single-crystal electrodes. We summarize the relevant reaction steps and observed products and intermediates in Fig. 13.

In alkaline media, Cu (111) reduces NO$_3^-$ to NO$_2^-$ at lower overpotentials than on Cu (100). However, Cu (100) reduces NO$_2^-$ further to NH$_2$OH with a considerably higher rate than Cu (111), reaching almost perfect diffusion limitation. Nitrite is observed as an intermediate of the reaction on both surfaces, but no other volatile or surface-adsorbed intermediates have been identified. Both Cu (100) and Cu (111) suffer from inhibition and deactivation by the concurrent hydrogen adsorption reaction. We attribute the deactivation to adsorbed hydrogen since it is not observed if the potential remains at values at which the HER does not occur. Cu (111) is more sensitive to this inhibition/deactivation than Cu (100) because the hydrogen evolution reaction is more active on Cu (111) and Cu (100), both in acidic and alkaline media. The higher activity of Cu (111) for HER as compared to Cu (100) is in agreement with recent theoretical predictions by Santos et al. [26].
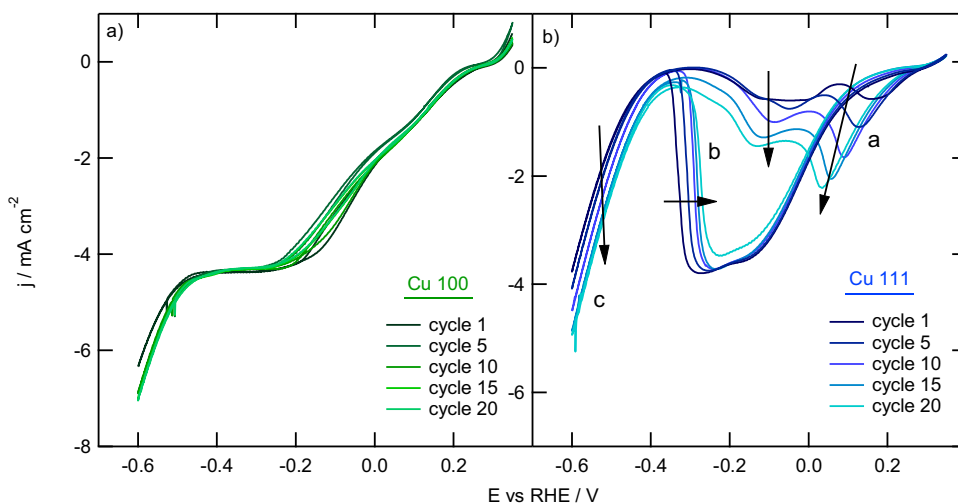
Fig. 10. Cyclic voltammetry recorded at a) Cu (100) and b) Cu (111) electrodes in 0.1 M HClO$_4$ in the presence of 2 mM NaNO$_3$ as a function of the number of cycles. Experimental conditions: scan rate 50 mV/s; rotation rate 400 rpm.

In acidic media, Cu (100) reduces NO$_3^-$ to HNO$_2$ at slightly lower potential than Cu (111). In acid media HNO$_2$ forms NO in solution [9] leading to NO$_{ads}$ on both Cu surfaces, which in turn is reduced to ammonium at roughly the same potential. The reduction of nitrate on Cu (100) is diffusion limited as in alkaline media, but the reduction does not seem to correspond to a single product. Irreversible deactivation is observed on Cu (111) in acidic media, due to the concomitant HER and the related formation of adsorbed hydrogen.

These results demonstrate that the most suitable copper surface for nitrate reduction is the Cu (100) surface, in terms of its activity, its ability to reduce nitrate to an interesting product (hydroxylamine) in alkaline media, and for its smaller tendency to deactivate due to its lower HER activity compared to Cu (111). Remarkably, the final product of nitrate reduction appears to be pH sensitive: ammonia in acidic media, hydroxylamine in alkaline media.
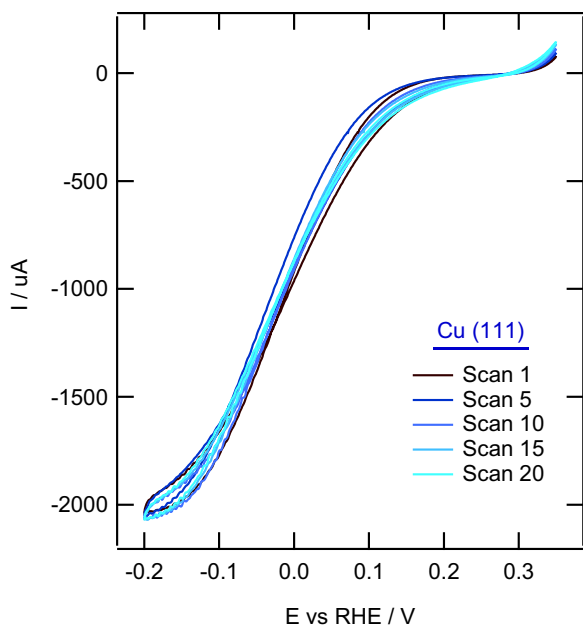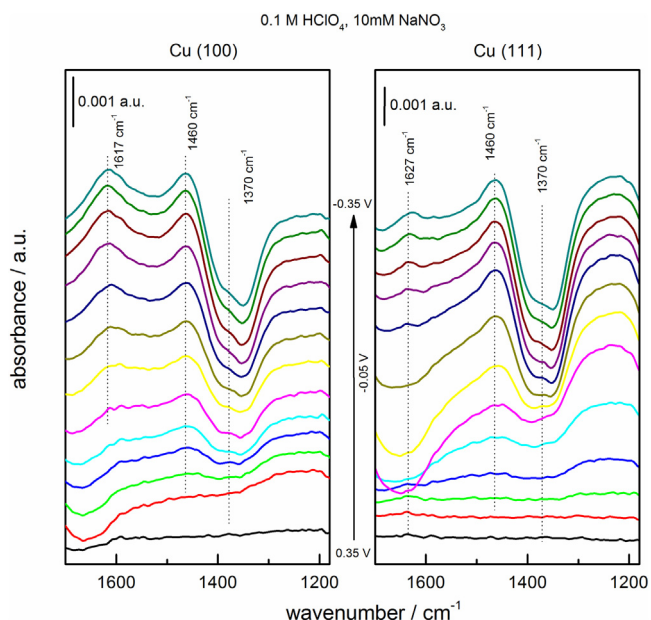

Fig. 12. Potential dependent absorbance spectra for the reduction of 10 mM NaNO$_3$ on Cu (100) (left panel) and on Cu (111) (right panel) electrode in 0.1 M HClO$_4$ solution. Reference spectrum recorded at 0.35 V vs. RHE.
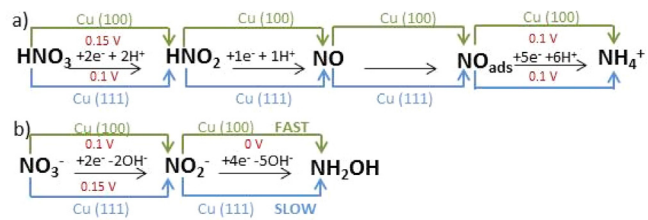

Fig. 13. Proposed mechanism for nitrate reduction on copper single crystals in a) acidic media and b) alkaline media.

4. Conclusions

Electrocatalytic reduction of nitrate on Cu single crystals has been investigated by electrochemical methods coupled with in situ

Fig. 11. Cyclic voltammetry recorded at a Cu (111) electrode in 0.1 M HClO$_4$ in the presence of 2 mM NaNO$_3$ as a function of the number of cycles. Experimental conditions: scan rate 50 mV/s; rotation rate 400 rpm.

and online analytical techniques, showing that the reduction of nitrate on copper single crystals is sensitive to both surface structure and pH. In alkaline media, Cu (111) reduces nitrate to nitrite at slightly lower potentials than Cu (100), but Cu (100) performs much better in reducing nitrite further to hydroxylamine. In acidic media, there are some differences in the CV profiles, but both copper electrodes give the same intermediates and products: NO, NO_{ads} and NH_4^+. In addition, deactivation of Cu (111) during the reduction of nitrate or nitrite has a larger effect than on Cu (100), in both alkaline and acidic electrolytes studied. The nature of the deactivation is presumably due to the formation of H_{ads} and the difference between the extent of deactivation of the two surfaces can be related to the higher hydrogen evolution activity of the Cu (111) electrode. Therefore, nitrate reduction on copper is a pH dependent reaction, forming NO and NH_4^+ when an acidic electrolyte is used, and NO_2^- and NH_2OH when the electrolyte is alkaline.

Acknowledgments

Appendix A. Supplementary data

Supplementary data associated with this article can be found, in the online version, at http://dx.doi.org/10.1016/j.electacta.2016.12.147.

References

[1] J.N. Galloway, W.H. Schlesinger, H. Levy, A. Michaels, J.L. Schnoor, Nitrogen fixation: Anthropogenic enhancement-environmental response, Global Biogeochemical Cycles 9 (1995) 235–252.

[2] P.M. Vitousek, R.W. Howarth, Nitrogen Limitation on Land and in the Sea: How Can It Occur? Biogeochemistry 13 (1991) 87–115.

[3] J.N. Galloway, A.R. Townsend, J.W. Erisman, M. Bekunda, Z. Cai, J.R. Freney, L.A. Martinelli, S.P. Seitzinger, M.A. Sutton, Transformation of the Nitrogen Cycle: Recent Trends, Questions, and Potential Solutions, Science 320 (2008) 889–892.

[4] M. Duca, B. van der Klugt, M. Koper, Electrocatalytic reduction of nitrite on transition and coinage metals, Electrochimica Acta 68 (2012) 32–43.

[5] M. Duca, M.T. Koper, Powering denitrification: the perspectives of electrocatalytic nitrate reduction, Energy & Environmental Science 5 (2012) 9726–9742.

[6] D. Reyter, D. Bélanger, L. Roué, Study of the electroreduction of nitrate on copper in alkaline solution, Electrochimica Acta 53 (2008) 5977–5984.

[7] G.E. Badea, Electrocatalytic reduction of nitrate on copper electrode in alkaline solution, Electrochimica Acta 54 (2009) 996–1001.

[8] K. Bouzek, M. Paidar, A. Sadilkova, H. Bergmann, Electrochemical reduction of nitrate in weakly alkaline solutions, Journal of Applied Electrochemistry 31 (2001) 1185–1193.

[9] M. Duca, V. Kavvadia, P. Rodriguez, S.C.S. Lai, T. Hoogenboom, M.T.M. Koper, New insights into the mechanism of nitrite reduction on a platinum electrode, Journal of Electroanalytical Chemistry 649 (2010) 59–68.

[10] S.-E. Bae, A.A. Gewirth, Differential reactivity of Cu (111) and Cu (100) during nitrate reduction in acid electrolyte, Faraday discussions 140 (2009) 113–123.

[11] K.J.P. Schouten, E.P. Gallent, M.T. Koper, The electrochemical characterization of copper single-crystal electrodes in alkaline media, Journal of Electroanalytical Chemistry 699 (2013) 6–9.

[12] A.H. Wonders, T.H.M. Housmans, V. Rosca, M.T.M. Koper, On-line mass spectrometry system for measurements at single-crystal electrodes in hanging meniscus configuration, Journal of Applied Electrochemistry 36 (2006) 1215–1221.

[13] J. Yang, Y. Kwon, M. Duca, M.T. Koper, Combining Voltammetry and Ion Chromatography: Application to the Selective Reduction of Nitrate on Pt and PtSn Electrodes, Analytical chemistry 85 (2013) 7645–7649.

[14] M.C. Figueiredo, J. Souza-Garcia, V. Climent, J.M. Feliu, Nitrate reduction on Pt (111) surfaces modified by Bi adatoms, Electrochemistry Communications 11 (2009) 1760–1763.

[15] S.-E. Bae, K.L. Stewart, A.A. Gewirth, Nitrate adsorption and reduction on Cu (100) in acidic solution, Journal of the American Chemical Society 129 (2007) 10171–10180.

[16] G. Dima, A. De Vooys, M. Koper, Electrocatalytic reduction of nitrate at low concentration on coinage and transition-metal electrodes in acid solutions, Journal of Electroanalytical Chemistry 554 (2003) 15–23.

[17] V. Rosca, M. Duca, M. de Groot, M.T. Koper, Nitrogen cycle electrocatalysis, Chemical Reviews 109 (2009) 2209–2244.

[18] O.A. Petrii, T.Y. Safonova, Electroreduction of nitrate and nitrite anions on platinum metals: a model process for elucidating the nature of the passivation by hydrogen adsorption, Journal of Electroanalytical Chemistry 331 (1992) 897–912.

[19] G. Horanyi, E. Rizmayer, Role of adsorption phenomena in the electrocatalytic reduction of nitric acid at a platinized platinum electrode, Journal of Electroanalytical Chemistry and Interfacial Electrochemistry 140 (1982) 347–366.

[20] M.T. Koper, Non-linear phenomena in electrochemical systems, Journal of the Chemical Society, Faraday Transactions 94 (1998) 1369–1378.

[21] V. Rosca, G.L. Beltramo, M.T.M. Koper, Hydroxylamine electrochemistry at polycrystalline platinum in acidic media: a voltammetric, DEMS and FTIR study, Journal of Electroanalytical Chemistry 566 (2004) 53–62.

[22] A. Rodes, R. Gomez, J. Orts, J. Feliu, A. Perez, A. Aldaz, In situ FTIR spectroscopy characterization of the NO adlayers formed at platinum single crystal electrodes in contact with acidic solutions of nitrite, Langmuir 11 (1995) 3549–3553.

[23] M. Hughes, H. Nicklin, K. Shrimanker, Autoxidation of hydroxylamine in alkaline solutions. Part II. Kinetics. The acid dissociation constant of hydroxylamine, Journal of the Chemical Society A: Inorganic, Physical, Theoretical (1971) 3485–3487.

[24] P. Dumas, M. Suhren, Y. Chabal, C. Hirschmugl, G. Williams, Adsorption and reactivity of NO on Cu (111): a synchrotron infrared reflection absorption spectroscopic study, Surface science 371 (1997) 200–212.

[25] C. Kim, C.-W. Yi, D. Goodman, Adsorption and reaction of NO on Cu (100): an infrared reflection absorption spectroscopic study at 25 K, The Journal of Physical Chemistry B 106 (2002) 7065–7068.

[26] E. Santos, K. Pötting, A. Lundin, P. Quaino, W. Schmickler, Hydrogen Evolution on Single-Crystal Copper and Silver: A Theoretical Study, ChemPhysChem 11 (2010) 1491–1495.